On the Origin of Asymmetric Interactions between Permeant Anions and the Cystic Fibrosis Transmembrane Conductance Regulator Chloride Channel Pore

Mohammad Fatehi, Chantal N. St. Aubin, and Paul Linsdell
Department of Physiology and Biophysics, Dalhousie University, Halifax, Nova Scotia B3H 1X5, Canada

ABSTRACT Single channel and macroscopic current recording was used to investigate block of the cystic fibrosis transmembrane conductance regulator (CFTR) Cl^- channel pore by the permeant anion $Au(CN)_2^-$. Block was 1–2 orders of magnitude stronger when $Au(CN)_2^-$ was added to the intracellular versus the extracellular solution, depending on membrane potential. A point mutation within the pore, T-338A, strongly decreased the asymmetry of block, by weakening block by intracellular $Au(CN)_2^-$ and at the same time strengthening block by external $Au(CN)_2^-$. Block of T-338A, but not wild-type, was strongest at the current reversal potential and weakened by either depolarization or hyperpolarization. In contrast to these effects, the T-338A mutation had no impact on block by the impermeant $Pt(NO_2)_4^{2-}$ ion. We suggest that the CFTR pore has at least two anion binding sites at which $Au(CN)_2^-$ and $Pt(NO_2)_4^{2-}$ block Cl^- permeation. The T-338A mutation decreases a barrier for $Au(CN)_2^-$ movement between different sites, leading to significant changes in its blocking action. Our finding that apparent blocker binding affinity can be altered by mutagenesis of a residue which does not contribute to a blocker binding site has important implications for interpreting the effects of mutagenesis on channel blocker effects.

INTRODUCTION

Understanding the mechanism of action of ion channels has been given a tremendous boost in recent years by the generation of direct structural information in the form of channel crystal structures (1,2). One of the most striking features of these structures has been the identification of multiple discrete permeant ion binding sites within the pores of both cation selective (3,4) and anion selective channels (5). Permeant ion binding within the pore is thought to be key to the function of ion channels, providing the link between ionic selectivity and rapid ion transport both in cation channels (1,6) and anion channels (7,8).

Although direct structural evidence for ion binding sites inside channel pores is a recent breakthrough, the existence of such sites has been postulated for decades based on biophysical evidence (9). Most useful in these studies have been high affinity probes of ion binding sites, such as Ba^{2+} in K^+ channels (10,11), Cd^{2+} in Ca^{2+} channels (6), and SCN^- in Cl^- channels (12). For example, SCN^- has been used to probe the functional properties of the cystic fibrosis transmembrane conductance regulator (CFTR) Cl^- channel pore (12,13) and also to identify key pore-forming amino acid residues that potentially contribute to anion binding sites inside the pore (14–17). More recently, pseudohalide anions (such as $Au(CN)_2^-$ and $Pt(NO_2)_4^{2-}$) that inhibit Cl^- permeation at relatively low concentrations have been used to probe the CFTR pore (8,18–21). The apparent affinity of $Au(CN)_2^-$ binding is affected by point mutations throughout the putative pore region (21–23); however, since $Au(CN)_2^-$ is highly permeant in CFTR (18) it is difficult to separate the effects of mutagenesis on $Au(CN)_2^-$ binding and permeation. $Au(CN)_2^-$ has also recently been used to modify irreversibly cysteine residues introduced into the CFTR pore by site-directed mutagenesis (24). The divalent pseudohalide $Pt(NO_2)_4^{2-}$ has also been used effectively to probe the CFTR pore, with one important distinction from $Au(CN)_2^-$ being that $Pt(NO_2)_4^{2-}$ is impermeant (19). Since $Pt(NO_2)_4^{2-}$ is able to enter the pore and interfere with Cl^- permeation when applied to either side of the membrane, it has been suggested that distinct anion binding sites must exist on either side of some barrier inside the pore that prevents $Pt(NO_2)_4^{2-}$ movement (19,25).

One amino acid residue that has been implicated in $Au(CN)_2^-$ binding in the CFTR pore is T-338 in the sixth transmembrane region (TM6). Thus, the point mutation T-338A significantly reduces the apparent affinity with which intracellular $Au(CN)_2^-$ inhibits Cl^- current through the channel (21). A number of studies have implicated this threonine residue as being involved in determining the single channel conductance (26) and anion selectivity (26,27) of the pore, perhaps by contributing to the narrowest region of the pore (8,26). Initially it was suggested, based on substituted cysteine accessibility mutagenesis, that the amino acid side chain at this position was not in contact with the aqueous lumen of the pore (28); however, more recent studies have shown that the side chain does in fact line the pore (24,29,30). There is some evidence that mutagenesis of T-338 affects the binding of both permeant (17,21,27) and blocking anions

Submitted August 15, 2006, and accepted for publication November 7, 2006.

Address reprint requests to Paul Linsdell, PhD, Dept. of Physiology and Biophysics, Dalhousie University, 5850 College St., Halifax, Nova Scotia B3H 1X5, Canada. Tel.: 902-494-2265; Fax: 902-494-1685; E-mail: paul.linsdell@dal.ca.

Chantal N. St. Aubin's present address is Dept. of Pharmacology, University of Alberta, Edmonton, Alberta, Canada.

0006-3495/07/02/1241/13 $2.00

doi: 10.1529/biophysj.106.095349

(31,32) within the pore. It has been suggested that T-338 contributes to the narrow, central region of the CFTR pore, which is the main determinant of selectivity between different permeant anions (reviewed by Linsdell (8)).

This work investigates the interaction between permeant and impermeant blocking ions and the CFTR pore. The complex effects of the T-338A mutant on channel block suggest that this important threonine residue forms a barrier to permeant anion movement inside the pore and that the existence of this barrier underlies asymmetric anion binding properties of the wild-type channel pore. In particular, our finding that mutagenesis of T-338 drastically alters the potency of $Au(CN)_2^-$ block apparently without directly affecting an anion binding site has important implications for studies that seek to identify blocker binding sites within ion channel pores using mutagenesis.

MATERIALS AND METHODS

Experiments were carried out on baby hamster kidney cells stably transfected with human wild-type or T-338A-CFTR, prepared as described previously (17). Macroscopic and single channel patch clamp recordings were made from inside out patches excised from these cells, as described in detail previously (21–33). After patch excision and recording of background currents, CFTR channels were activated by exposure to protein kinase A (PKA) catalytic subunit plus MgATP (1 mM) in the cytoplasmic (bath) solution. As in a previous study (22), single channel currents were recorded after weak PKA stimulation (1–10 nM), whereas all macroscopic CFTR currents were recorded after maximal PKA stimulation (~20 nM) and subsequent treatment with sodium pyrophosphate (PPi, 2 mM) to ''lock'' channels in the open state. Because single channel activity was recorded under conditions of weak PKA stimulation, patches contained a large number of CFTR channels with very low open probability, and as a result no information is contained in the relative open probability under different ionic conditions. Both intracellular (bath) and extracellular (pipette) solutions were based on one containing (in mM): 150 NaCl, 10 *N*-Tris[hydroxymethyl]methyl-2-aminoethanesulfonate (TES), 2 $MgCl_2$, pH 7.4, to which $KAu(CN)_2$ (3 μM–10 mM), $K_2Pt(NO_2)_4$ (1 mM), or NaSCN (10 mM) was added as necessary. To study the effects of changing Cl^- concentration on block by $Au(CN)_2^-$ (see Fig. 9), the NaCl concentration in either the intracellular or extracellular solution was reduced to 20 mM by replacement with glucose. In these experiments, membrane voltages were corrected for liquid junction potentials calculated using pCLAMP9 software (Molecular Devices, Sunnyvale, CA). All chemicals were from Sigma (Oakville, ON, Canada) except PKA (Promega, Madison, WI) and $K_2Pt(NO_2)_4$ (Strem Chemicals, Newburyport, MA).

Current traces were filtered at 50 Hz (for single channel currents) or 100–200 Hz (for macroscopic currents) using an eight-pole Bessel filter, digitized at 250 Hz–1 kHz, and analyzed using pCLAMP9 software (Molecular Devices). Single channel current amplitudes were estimated from all-points amplitude histograms (e.g., Fig. 1, *B* and *C*). Macroscopic current-voltage (I/V) relationships were constructed using depolarizing voltage ramp protocols, with a rate of change of voltage of 100–125 mV s^{-1} (34,35). Background (leak) currents recorded before the addition of PKA were subtracted digitally, leaving uncontaminated CFTR currents (19,35). Macroscopic chord conductance (G) was estimated at different voltages by dividing the current by the driving force (membrane potential minus current reversal potential; the reversal potential was 0 mV in all cases) and is plotted as a fraction of maximal chord conductance (G_{MAX}) (see Fig. 5 *B*).

Concentration-inhibition relationships were fitted by the equation

$$\text{fractional unblocked current} = 1/(1 + ([B]/K_d)), \qquad (1)$$

where [B] is the blocker concentration and K_d its apparent dissociation constant.

Energy barrier profiles based on transition rate theory were constructed using the AJUSTE computer program developed by Alvarez et al. (36) and used previously to model anion permeation and block in the CFTR pore (13,37). Two models were developed, in which the pore was assumed to have either one or two binding sites for permeant anions (Cl^- and $Au(CN)_2^-$). Adjustable parameters during the fitting procedure were the energies for both Cl^- and $Au(CN)_2^-$ ions at the energy minima (wells) and maxima (peaks). For simplicity and to minimize the number of adjustable parameters, wells and peaks in the one-site model were fixed at values described in a previous study (13), and in the two-site model wells and peaks were fixed at regular intervals within the transmembrane electric field. Other details of the modeling procedure are as described previously (13,36,37).

Throughout, mean data are presented graphically with error bars reflecting mean ± SE; where no error bars are shown, this error is smaller than the size of the symbol. Statistical comparisons between groups of data were carried out using Student's two-tailed *t*-test, with $P < 0.05$ being considered statistically significant.

RESULTS

Asymmetric block of wild-type CFTR by $Au(CN)_2^-$ ions

$Au(CN)_2^-$ ions have previously been shown by our lab (19,38) and others (24) to cause a reduction in the amplitude of unitary CFTR Cl^- channel current, due to its ability to bind within the pore with high affinity and interrupt the flow of Cl^- ions. However, although $Au(CN)_2^-$ is highly permeant in CFTR (18,21) and can inhibit CFTR Cl^- currents from either side of the membrane (24), its inhibitory effects have previously been studied at the single channel level only when present in the intracellular solution (19,24,38). Fig. 1 shows the block of unitary CFTR Cl^- currents recorded in inside out membrane patches by both intracellular and extracellular $Au(CN)_2^-$. As reported previously (24,38), intracellular $Au(CN)_2^-$ caused a voltage-dependent block of unitary Cl^- current at concentrations below 1 mM (Fig. 1, *A–D*). However, very much higher concentrations of $Au(CN)_2^-$ were required in the extracellular solution to produce comparable levels of inhibition (Fig. 1, *A–C* and *E*). This asymmetry of blocking action is seen more clearly from single channel concentration-inhibition curves shown in Fig. 2 *A*. These curves further demonstrate that, unlike intracellular $Au(CN)_2^-$, extracellular $Au(CN)_2^-$ exhibits little or no voltage dependence of block. Fits to these curves by Eq. 1 were used to estimate the apparent affinity of $Au(CN)_2^-$ block; results of these fits are shown in Fig. 2 *B*. $Au(CN)_2^-$ inhibits unitary Cl^- current with significantly (~1–2 orders of magnitude) lower affinity when present in the extracellular versus the intracellular solution, depending on the membrane potential. Thus, despite its high permeability in the CFTR pore, $Au(CN)_2^-$ shows highly asymmetric blocking effects on Cl^- movement through the pore.

Block of T-338A-CFTR by $Au(CN)_2^-$

We also investigated $Au(CN)_2^-$ block of unitary currents in T-338A-CFTR. As described in the introduction, this mutant

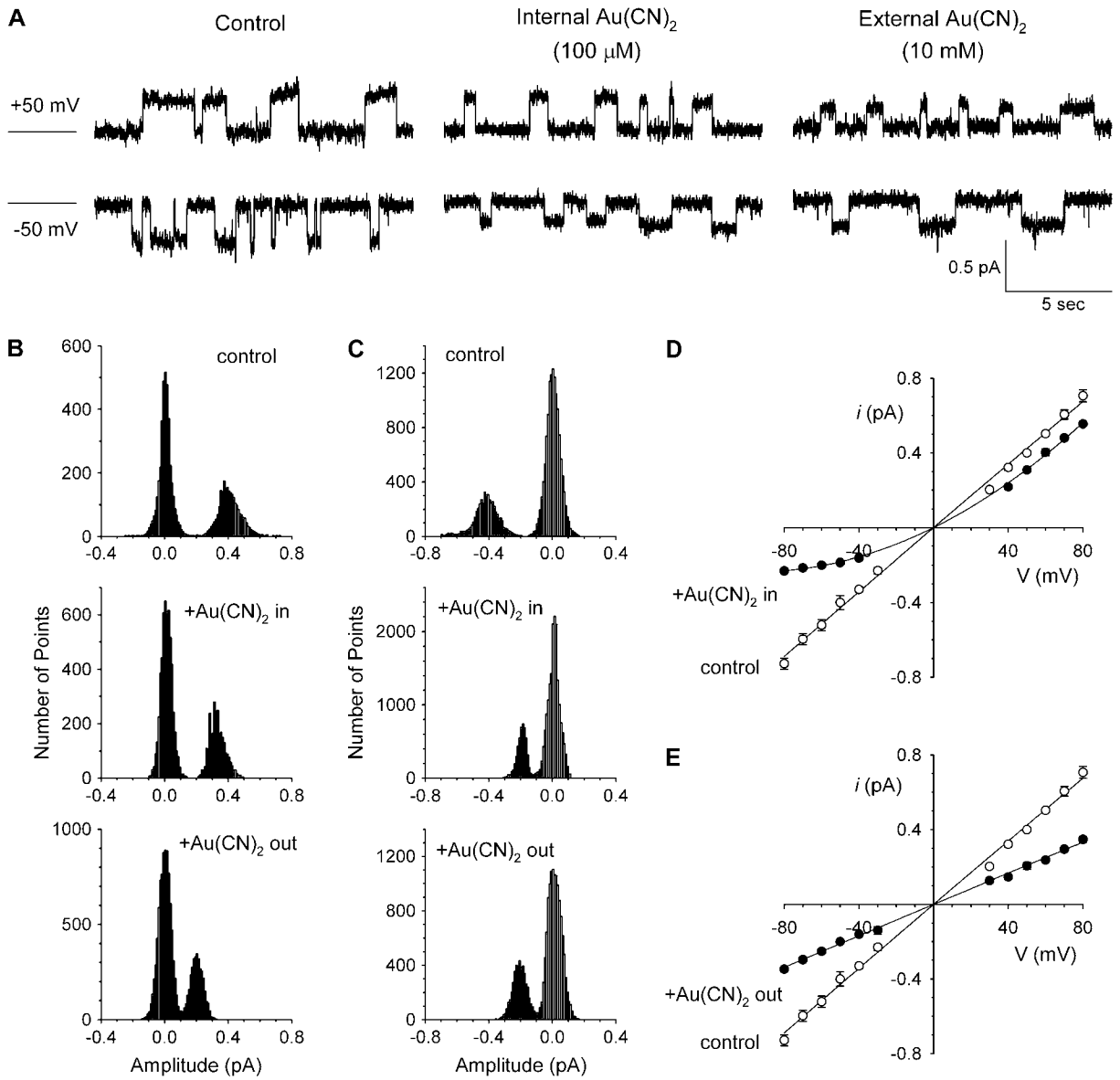

FIGURE 1 Asymmetric block of wild-type CFTR by $Au(CN)_2^-$ ions. (*A*) Example single channel currents recorded from inside out patches at membrane potentials of +50 mV and −50 mV, as indicated. In each case the closed state of the channel is indicated by the line on the far left. Currents were recorded in the absence of $Au(CN)_2^-$ (control) or with $Au(CN)_2^-$ present in the intracellular solution (100 μM) or the extracellular solution (10 mM). In both cases $Au(CN)_2^-$ causes a reduction in unitary current amplitude, as further demonstrated from amplitude histograms prepared from these current traces at +50 mV (*B*) and −50 mV (*C*) and also from mean unitary current-voltage relationships recorded under these conditions (*D* and *E*). Mean of data from 3–5 patches in *D* and *E*.

has been shown to exhibit elevated unitary Cl^- conductance (26), increased $Au(CN)_2^-$ permeability (21), and weakened block by intracellular $Au(CN)_2^-$ at the macroscopic current level (21,22). The effects of intracellular and extracellular $Au(CN)_2^-$ on wild-type and T-338A-CFTR single channel currents are compared in Fig. 3. These traces indicate that, whereas the inhibitory effects of 100 μM intracellular $Au(CN)_2^-$ are weakened in T-338A, the inhibitory effects of 1 mM extracellular $Au(CN)_2^-$ are enhanced in this mutant.

$Au(CN)_2^-$ block of T-338A-CFTR unitary currents is explored in more detail in Fig. 4. Unitary current-voltage relationships recorded in the presence of the same concentration of $Au(CN)_2^-$ (1 mM) in either the intracellular or extracellular solution are shown in Fig. 4 *A*. The unitary current-voltage relationship recorded in the presence of extracellular $Au(CN)_2^-$ shows an unusual ''N''-shape, suggesting that block is stronger close to 0 mV than at either strongly hyperpolarized or strongly depolarized membrane potentials (Fig. 4 *A*). In the presence of intracellular $Au(CN)_2^-$, the current-voltage relationship appears linear at hyperpolarized voltages but outwardly rectified at depolarized voltages (Fig. 4 *A*). The concentration dependence of $Au(CN)_2^-$ block

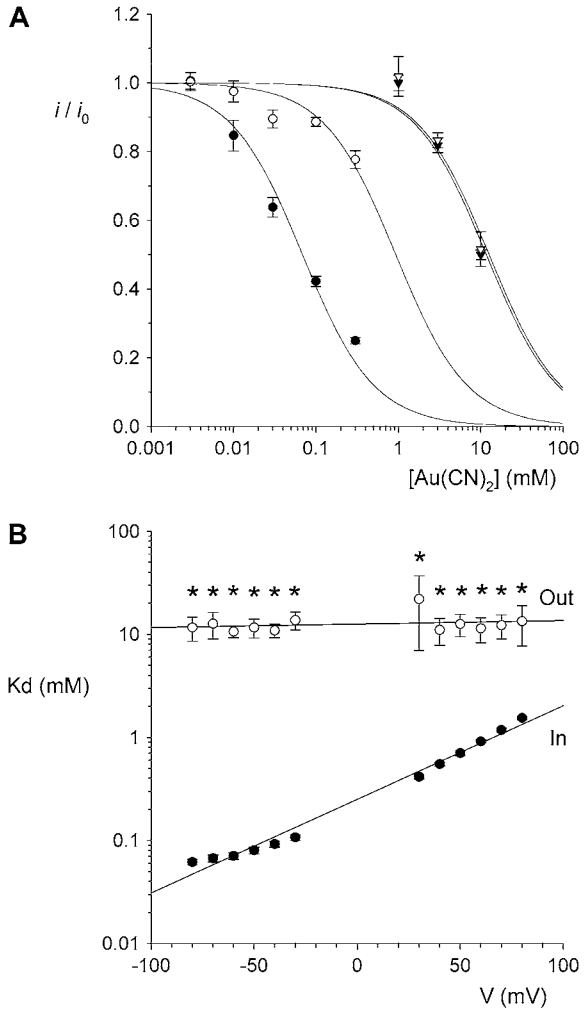

FIGURE 2 Concentration and voltage dependence of block by $Au(CN)_2^-$ ions. (*A*) Fractional unitary current remaining (i/i_0) after addition of different concentrations of $Au(CN)_2^-$ to the intracellular or extracellular solution: (●) internal $Au(CN)_2^-$, −50 mV; (○) internal $Au(CN)_2^-$, +50 mV; (▼) external $Au(CN)_2^-$, −50 mV; (∇) external $Au(CN)_2^-$, +50 mV. Each of these four sets of data has been fitted by Eq. 1. (*B*) Mean K_d calculated from curves such as those shown in (*A*) for both internal (●) and external (○) $Au(CN)_2^-$. Mean of data from 3–5 patches. Asterisks indicate a statistically significant difference from the K_d for internal $Au(CN)_2^-$.

of T-338A single channel currents is shown in Fig. 4, *B* and *C*. The apparent affinity of block is similar for both internal and external $Au(CN)_2^-$, and in both cases the apparent K_d is minimal close to 0 mV and increases with either hyperpolarization or depolarization of the membrane potential (Fig. 4 *C*). The unusual ''U''-shaped voltage dependence of apparent blocker affinity for external $Au(CN)_2^-$ is a consequence of the ''N''-shaped unitary current-voltage relationship (Fig. 4 *A*), and the slight ''U''-shape also seen with internal $Au(CN)_2^-$ (Fig. 4 *C*) hints at a similar, perhaps less pronounced, biphasic voltage dependence of block. To confirm this unusual current-voltage relationship shape, we recorded macroscopic T-338A current-voltage relationships over extended voltage ranges (−100 to +100 mV) in the absence of $Au(CN)_2^-$ or with $Au(CN)_2^-$ in the internal (2 mM) or external (1 mM) solutions, after maximal channel activation with PKA and ATP and subsequent channel ''locking open'' with PPi. As shown in Fig. 5 *A*, under these conditions T-338A-CFTR exhibits an almost completely linear macroscopic current-voltage relationship over the voltage range −100 to +100 mV, which, due to the locking of channels in the open state, should reflect the open channel unitary current-voltage relationship. In the presence of $Au(CN)_2^-$ in either the intracellular or extracellular solution; however, the macroscopic current-voltage relationship shows an ''N''-shape (Fig. 5 *A*) reminiscent of the shape of the unitary current-voltage relationships in the presence of $Au(CN)_2^-$ (Fig. 4 *A*). Quantification of the relative chord conductance at different membrane potentials indicates that, under control conditions, conductance in T-338A is maximal around 0 mV and decreases very slightly at strongly hyperpolarized and strongly depolarized membrane potentials (Fig. 5 *B*). In contrast, in the presence of both intracellular and extracellular $Au(CN)_2^-$ conductance is minimal close to 0 mV and increases greatly when the membrane potential is hyperpolarized or depolarized (Fig. 5 *B*). By analogy with the single channel current-voltage relationships and voltage dependence of K_d shown in Fig. 4, this reflects strong block by both intracellular and extracellular $Au(CN)_2^-$ at 0 mV and relief of block by both hyperpolarization and depolarization of the membrane potential.

The inhibitory effects of intracellular and extracellular $Au(CN)_2^-$ on wild-type and T-338A-CFTR are compared directly in Fig. 6. These data show that the T-338A mutation significantly decreases the apparent affinity of block by intracellular $Au(CN)_2^-$ (especially at hyperpolarized membrane potentials where the block of wild-type is strongest) while significantly increasing the apparent affinity of block by extracellular $Au(CN)_2^-$.

Block of T-338A-CFTR by other small anions

We hypothesized that the dramatic weakening of the asymmetry of $Au(CN)_2^-$ block that we observed in T-338A-CFTR was related to the fact that $Au(CN)_2^-$ is a permeant blocker of the channel pore (18,21). We therefore wondered if the T-338A mutation would affect the apparent affinity of block by small anions that act as open channel blockers but that are impermeant. One such anion is the divalent pseudohalide ion $Pt(NO_2)_4^{2-}$, which is impermeant but can block the channel from either the intracellular and extracellular side of the membrane (19,25). Indeed, we have previously shown by macroscopic current recording that the T-338A mutation does not significantly affect block by intracellular $Pt(NO_2)_4^{2-}$ (19). To investigate the blocking effects of extracellular $Pt(NO_2)_4^{2-}$ we used single channel recording from inside out membrane patches in the absence or presence of $Pt(NO_2)_4^{2-}$ in the extracellular solution (Fig. 7). Unitary current-voltage relationships recorded under these conditions (Fig. 7 *B*),

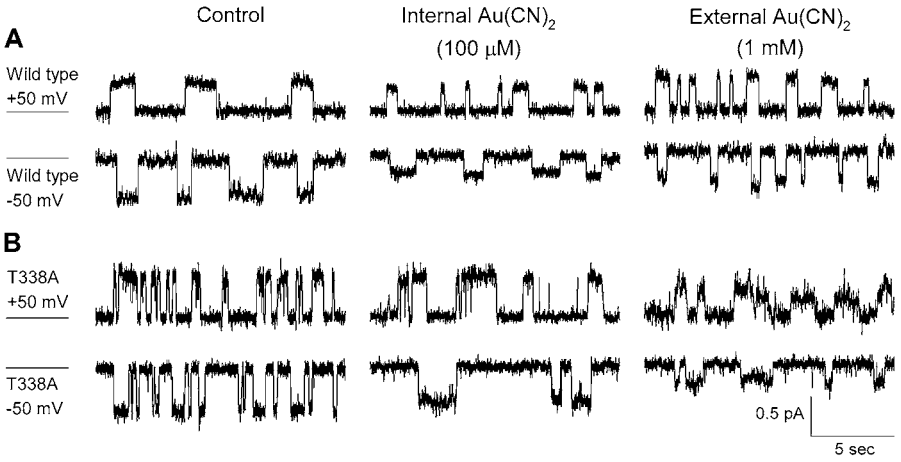

FIGURE 3 Both internal and external $Au(CN)_2^-$ block are altered in T-338A-CFTR. Example single channel currents for wild-type (*A*) and T-338A-CFTR (*B*) recorded from inside out patches at membrane potentials of +50 mV and −50 mV, as indicated. In each case the closed state of the channel is indicated by the line on the far left. Currents were recorded in the absence of $Au(CN)_2^-$ (control) or with $Au(CN)_2^-$ present in the intracellular solution (100 μM) or the extracellular solution (1 mM).

as well as the fractional current observed in the presence of 1 mM $Pt(NO_2)_4^{2-}$ (Fig. 7 *C*), indicate that $Pt(NO_2)_4^{2-}$ causes a strongly voltage-dependent inhibition of unitary current amplitude that appears similar in both wild-type and T-338A-CFTR.

Unitary Cl^- current in wild-type CFTR is also blocked by another permeant anion, SCN^- (13), albeit with a considerably lower affinity than that observed for $Au(CN)_2^-$. However, although SCN^- shows a fairly similar permeability to $Au(CN)_2^-$ (12,18,21), its blocking effects are quite symmetrical, with an ~2-fold higher K_d having been reported for extracellular SCN^- block of unitary Cl^- currents (14.2 mM at 0 mV membrane potential) compared to intracellular SCN^- (6.2 mM at 0 mV) (13). Since one of the most striking effects of the T-338A mutation was the weakening of the asymmetry of $Au(CN)_2^-$ block, we also wondered how this mutation would affect the already quite symmetrical blocking effects of SCN^-. As shown in Fig. 8, *A* and *B*, 10 mM SCN^- had broadly similar blocking effects on T-338A unitary Cl^- currents when present in either the intracellular or extracellular solution. As with $Au(CN)_2^-$ block, the unitary current-voltage relationship in the presence of SCN^- was noticeably ''N''-shaped (Fig. 8 *B*). As a result, the voltage dependence of block, like that of $Au(CN)_2^-$, showed a ''U''-shape, with strongest inhibition close to 0 mV (Fig. 8, *C* and *D*). Whereas SCN^- caused a similar degree of inhibition of wild-type CFTR (13) (Fig. 8, *C* and *D*), the voltage dependence of block was more conventional, with intracellular SCN^- blocking most strongly at hyperpolarized membrane potentials (Fig. 8 *C*) and extracellular SCN^- blocking most strongly at depolarized potentials (Fig. 8 *D*).

Origin of the voltage dependence of $Au(CN)_2^-$ block of T-338A-CFTR

A striking feature of T-338A-CFTR block by both $Au(CN)_2^-$ and SCN^- is the ''N''-shaped current-voltage relationship in the presence of blocker (Figs. 4 *A*, 5 *A*, and 8 *B*), reflecting a blocking event that is strongest close to 0 mV and is weakened by both hyperpolarization and depolarization. To investigate whether this reflected dependence of block on voltage itself or on the rate of Cl^- movement through the pore, we investigated block of T-338A-CFTR macroscopic currents by intracellular $Au(CN)_2^-$ in the presence of different transmembrane Cl^- concentration gradients (Fig. 9). Whether Cl^- was reduced to 20 mM in either the intracellular or extracellular solution, current inhibition by addition of 1 mM $Au(CN)_2^-$ was still associated with an ''N''-shaped current-voltage relationship (Fig. 9 *A*). As a result, maximal current inhibition occurred close to the current reversal potential (Fig. 9 *B*) under all ionic conditions studied. This suggests that voltage-dependent Cl^- movement through the pore—rather than membrane potential per se—is responsible for the weakening of $Au(CN)_2^-$ inhibition at extreme membrane potentials that results in the ''N''-shaped current-voltage relationships observed.

Rate theory models of $Au(CN)_2^-$ interaction with wild-type and T-338A-CFTR

To illustrate how the T-338A mutation might decrease the apparent affinity of block by internal $Au(CN)_2^-$ and yet increase the apparent affinity of block by external $Au(CN)_2^-$, we used the single channel I/V relationships shown in Figs. 1 and 4 to develop simple rate theory models of the CFTR pore. As described in the Discussion, our results could reflect either one or two $Au(CN)_2^-$ binding sites in the pore, and to reflect this we have developed two models, with either one or two anion binding sites (energy wells) within the pore. Best fit energy profiles for both Cl^- and $Au(CN)_2^-$ were simultaneously optimized by the fitting procedure, and the effects of the T-338A mutation were modeled by altering a single parameter—i.e., by lowering one energy barrier for both Cl^- and $Au(CN)_2^-$ movement in the pore (see Discussion). Relative energies for the two different anions are shown graphically as energy barrier profiles in Fig. 10, *A–D*. The predictions

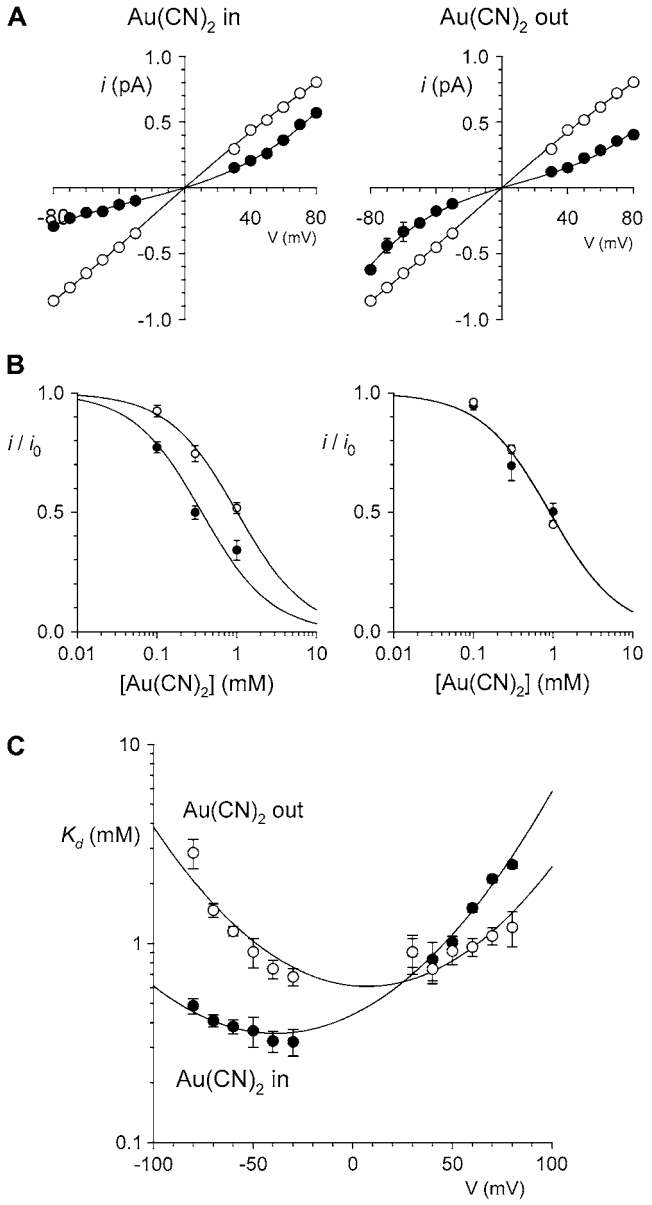

FIGURE 4 Concentration- and voltage dependence of block of T-338A-CFTR by $Au(CN)_2^-$ ions. (*A*) Mean unitary current-voltage relationships for T-338A-CFTR, under control conditions (○) and in the presence of 1 mM $Au(CN)_2^-$ (●) in the intracellular (*left*) or extracellular (*right*) solution. (*B*) Fractional unitary current remaining (i/i_0) after addition of different concentrations of $Au(CN)_2^-$ to the intracellular (*left*) or extracellular (*right*) solution, at membrane potentials of −50 mV (●) and +50 mV (○). Each of these four sets of data has been fitted by Eq. 1. (*C*) Mean K_d calculated from curves such as those shown in *B* for both internal (●) and external (○) $Au(CN)_2^-$. Mean of data from 3–8 patches in each panel.

of the models (Fig. 10, *E–H*) indicate that both the single binding site model (Fig. 10, *A* and *B*) and the two binding site model (Fig. 10, *C* and *D*) are able to replicate the most salient features observed experimentally—strong block of wild-type by internal $Au(CN)_2^-$, weak block of wild-type by external $Au(CN)_2^-$, weakened block of T-338A by internal $Au(CN)_2^-$, and yet strengthened block of this mutant by external $Au(CN)_2^-$.

DISCUSSION

$Au(CN)_2^-$ is an asymmetric blocker of the wild-type CFTR channel pore

Inhibition of wild-type CFTR by $Au(CN)_2^-$ has been investigated in many previous studies (18,21,24,33,38). When applied to the cytoplasmic face of inside out membrane patches, $Au(CN)_2^-$ has two inhibitory effects on CFTR Cl^- currents—a high affinity reduction in channel open probability, and a lower affinity, voltage-dependent reduction in unitary current amplitude (38). This second effect appears to reflect binding of $Au(CN)_2^-$ within the open channel pore, where it impedes Cl^- movement through the pore. External $Au(CN)_2^-$ has been reported to inhibit wild-type CFTR with a broadly similar potency and probably by the same mechanism (18,24); however, these effects have been observed only at the whole cell current level. It is somewhat surprising, therefore, that the effects of $Au(CN)_2^-$ on CFTR single channel current amplitude show such strong asymmetry—with external $Au(CN)_2^-$ being 1–2 orders of magnitude lower affinity than intracellular $Au(CN)_2^-$ (Fig. 2). Thus the inhibitory effects of extracellular $Au(CN)_2^-$ that we observe at the single channel level (Fig. 1)—which suggest a K_d of ~10 mM (Fig. 2)—appear to be much weaker than those reported using whole cell recording (18,24). This discrepancy may reflect multiple inhibitory effects of extracellular $Au(CN)_2^-$ that contribute to the overall inhibition observed at the whole cell level—a situation analogous to the multiple inhibitory effects of intracellular $Au(CN)_2^-$ that contribute to its blocking actions on macroscopic Cl^- currents (38). Thus it is possible (but not investigated) that external $Au(CN)_2^-$ could affect the open probability of the channel; it has been shown previously that CFTR gating is sensitive to extracellular anions including Cl^- itself (39). It is less likely that $Au(CN)_2^-$ is permeating the channel to inhibit channel open probability at an intracellular site of action, since the inhibitory effects of external $Au(CN)_2^-$ on whole cell currents have been shown to be readily reversible (24). Irrespective of the reasons for these discrepancies, the strikingly different effects of $Au(CN)_2^-$ on single channel current amplitude suggest that $Au(CN)_2^-$ ions bind much more tightly inside the pore when added to the intracellular versus the extracellular solution.

Why is $Au(CN)_2^-$ block of Cl^- permeation through the pore so strongly asymmetric? It is well known that large organic anions usually block the CFTR channel pore only from the inside, due primarily to their interaction with a positively charged amino acid side chain (K-95 in TM1) in the wide inner vestibule of the pore (40–42). These large substances are thought to be excluded from the extracellular mouth of the pore for reasons related to their size (43). In

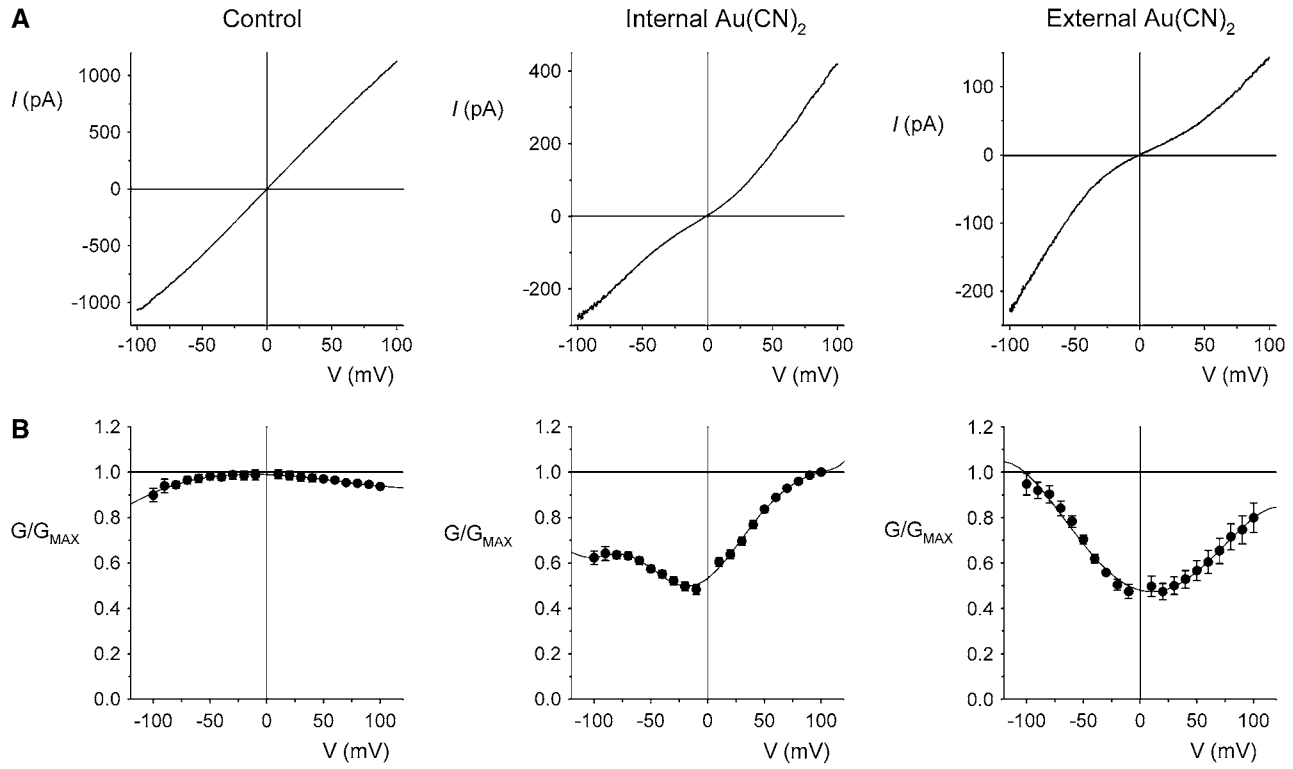

FIGURE 5 Macroscopic currents demonstrate the unusual voltage dependence of $Au(CN)_2^-$ block of T-338A-CFTR. (*A*) Example leak-subtracted current-voltage (I/V) relationships recorded from inside out membrane patches after maximal current stimulation with PKA and PPi. Currents were recorded in the absence of $Au(CN)_2^-$ (*left*), with 2 mM $Au(CN)_2^-$ present in the intracellular solution (*center*), or with 1 mM $Au(CN)_2^-$ in the extracellular solution (*right*). (*B*) Quantification of the shape of the I/V curve under these conditions. The chord conductance at different voltages, relative to the maximum chord conductance (G/G_{MAX}), was estimated as described in Materials and Methods. Mean of data from 4–5 patches.

contrast, $Au(CN)_2^-$ is highly permeant in CFTR (in fact, with a higher permeability than Cl^- itself) (18,21), such that it is expected to have access to binding sites throughout the pore when present in either the intracellular or the extracellular solution. Nevertheless, its interactions with binding sites within the pore appear to be very different depending on which side of the membrane it is applied from. This could reflect either a single $Au(CN)_2^-$ binding site in the pore that is more accessible from the intracellular solution or separate binding sites that underlie block by intracellular and extracellular $Au(CN)_2^-$, with the intracellular site showing a greater affinity for $Au(CN)_2^-$. Currently we do not have enough information to be able to discriminate between these two models, and as a result we have developed rate theory models having either one or two binding sites (energy wells). Indeed, the energy profiles generated for wild-type CFTR reflect the general features described above; the single site model (Fig. 10 *A*) shows a lower energy barrier (resulting in easier access) for $Au(CN)_2^-$ entry from the intracellular side of the membrane, whereas the two-site model (Fig. 10 *C*) shows a deeper energy well (resulting in tighter binding) for the more cytoplasmically located binding site. Although we find that the single binding site model is the simplest that can reproduce our single channel data (Fig. 10, *D* and *E*), there are several factors that we consider as favoring the second model with two binding sites. First, we believe that there are blocker binding sites in both the outer and inner mouths of the pore, since the impermeant anion $Pt(NO_2)_4^{2-}$ can block Cl^- permeation when added to either side of the membrane, apparently by binding to different sites (19,25). This is also consistent with the presence of a blocker binding site in the outer pore vestibule proposed by Muanprasat et al. (44). Second, point mutations in both the extracellular and intracellular mouths of the pore affect $Au(CN)_2^-$ block, and this may reflect disruption of separate binding sites. Thus, $Au(CN)_2^-$ block is greatly weakened by mutagenesis of R-334 (in TM6) (22,23), a positively charged residue which is involved in attracting extracellular Cl^- ions into the outer mouth of the pore (45), and of K-95 (in TM1) (22), the positive charge of which attracts intracellular Cl^- ions into the wide inner pore vestibule (40). Finally, block by extracellular $Au(CN)_2^-$ is apparently voltage independent (Fig. 2 *B*); although the voltage dependence of intracellular $Au(CN)_2^-$ block is complex in origin (33), this lack of voltage dependence would at first glance appear inconsistent with extracellular $Au(CN)_2^-$ ions moving deeply into the pore to block at a binding site located in the inner pore vestibule (Fig. 10 *A*).

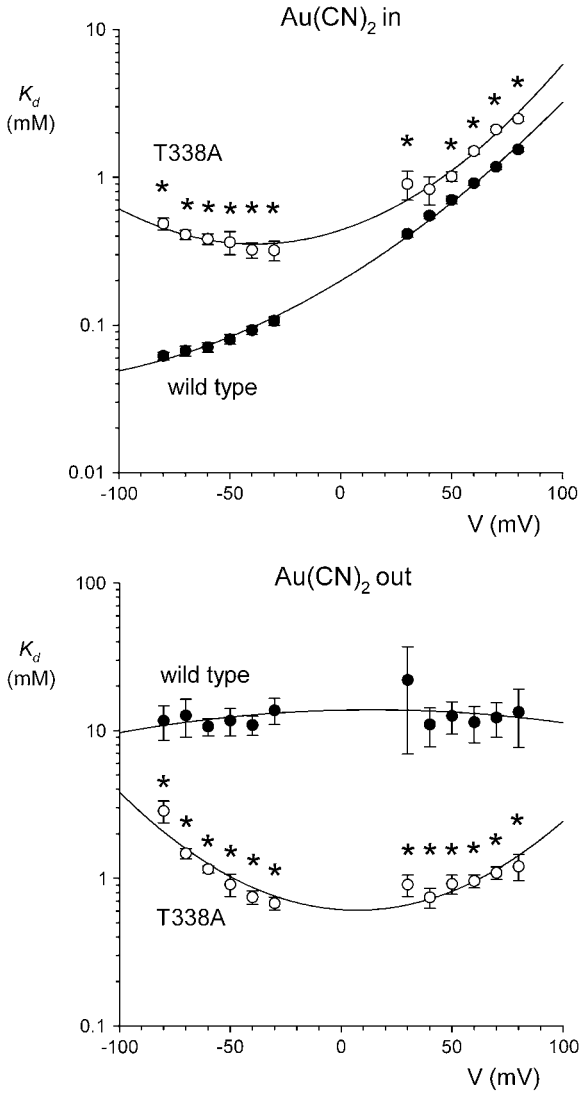

FIGURE 6 Comparison of the blocking effects of internal and external $Au(CN)_2^-$ ions between wild-type and T-338A-CFTR. Mean K_ds for wild-type (●) are as shown in Fig. 2 *B*; those for T-338A (○) are as in Fig. 4 *C*. In each case, asterisks indicate a statistically significant difference from wild-type.

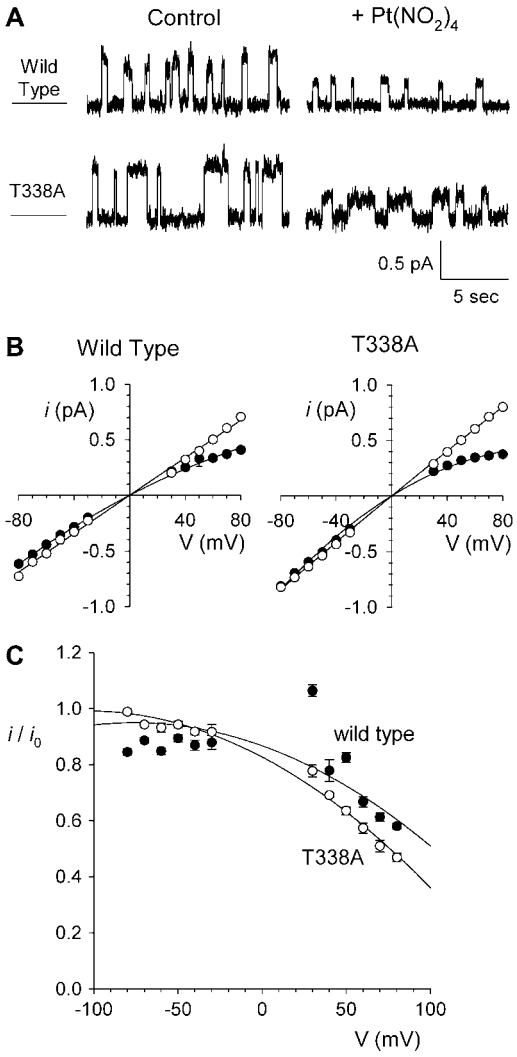

FIGURE 7 Block by external $Pt(NO_2)_4^{2-}$ ions. (*A*) Example single channel currents for wild-type and T-338A-CFTR recorded from inside out patches at a membrane potential of +70 mV, under control conditions (*left*) and in the presence of 1 mM $Pt(NO_2)_4^{2-}$ in the extracellular solution (*right*). (*B*) Mean unitary current-voltage relationships for wild-type and T-338A-CFTR, under control conditions (○) and in the presence of 1 mM $Pt(NO_2)_4^{2-}$ in the extracellular solution (●). (*C*) Fractional unitary current remaining in the presence of 1 mM extracellular $Pt(NO_2)_4^{2-}$. Mean of data from 3–5 patches in each panel.

$Au(CN)_2^-$ block of the T-338A-CFTR channel pore is much more symmetrical

Previously we showed, using macroscopic current recording, that block by intracellular $Au(CN)_2^-$ was greatly weakened in T-338A-CFTR and suggested that T-338 may contribute to a lyotropic anion binding site in the pore (21,22). However, the results here at the single channel level indicate that whereas this mutation does weaken block by intracellular $Au(CN)_2^-$, it actually strengthens block by extracellular $Au(CN)_2^-$ (Fig. 6). This apparently contradictory effect of a single mutation is difficult to reconcile with disruption of an $Au(CN)_2^-$ binding site in the pore. Instead, we now propose that the T-338A mutation alters the movement of $Au(CN)_2^-$ within the pore, changing its ability to access one or more binding sites the properties of which are not directly affected by the mutation. Consistent with this idea, block by impermeant $Pt(NO_2)_4^{2-}$ ions is not affected by the T-338A mutation, whether $Pt(NO_2)_4^{2-}$ is added to the intracellular (19) or extracellular solution (Fig. 7). This suggests that $Pt(NO_2)_4^{2-}$ ions are restricted to binding sites on the same side of the membrane to which they are applied and that the T-338A mutation has no impact either on the $Pt(NO_2)_4^{2-}$ binding affinity of these sites or on $Pt(NO_2)_4^{2-}$ movement between these sites.

The ways in which the T-338A mutation affects $Au(CN)_2^-$ inhibition can be interpreted in terms of either the single or

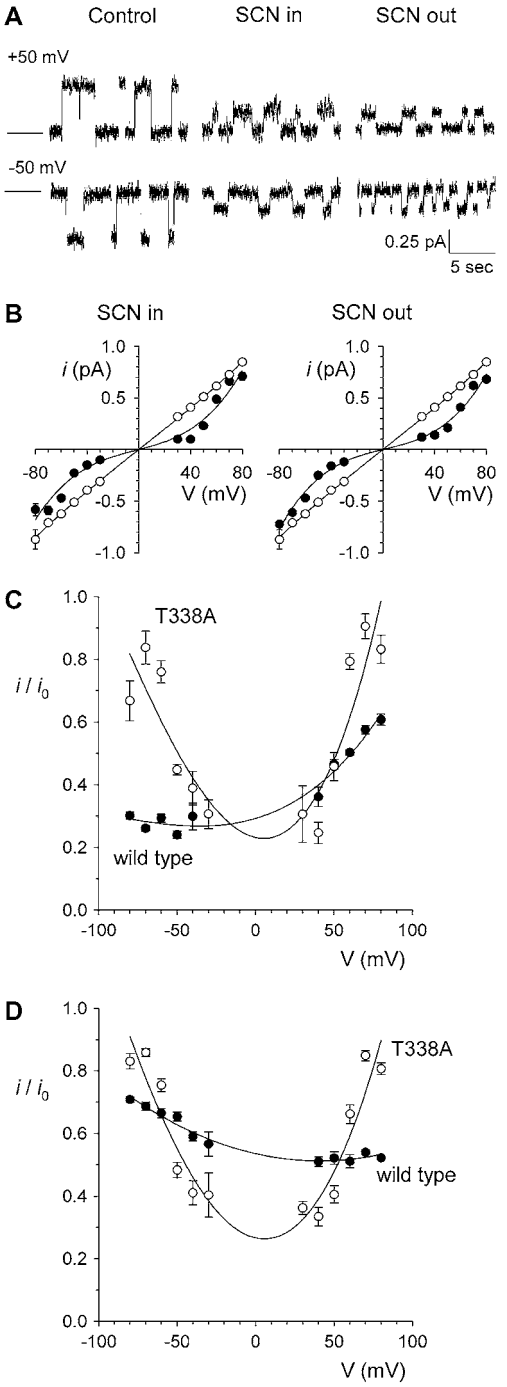

FIGURE 8 Block of T-338A-CFTR by internal and external SCN^- ions. (*A*) Example single channel currents for T-338A-CFTR, recorded from inside out patches at membrane potentials of +50 mV or −50 mV, under control conditions and in the presence of 10 mM SCN^- in the intracellular or extracellular solution, as indicated. (*B*) Mean unitary current-voltage relationships for T-338A-CFTR, under control conditions (○) and in the presence of 10 mM SCN^- (●) in the intracellular (*left*) or extracellular (*right*) solution. Mean of data from 3–10 patches. (*C*) Fractional unitary current remaining in the presence of 10 mM intracellular SCN^- for wild-type (●) and T-338A (○). (*D*) Fractional unitary current remaining in the presence of 10 mM extracellular SCN^- for wild-type (●) and T-338A (○). In *C* and *D*, data for wild-type are taken from Linsdell (13) under identical ionic conditions.

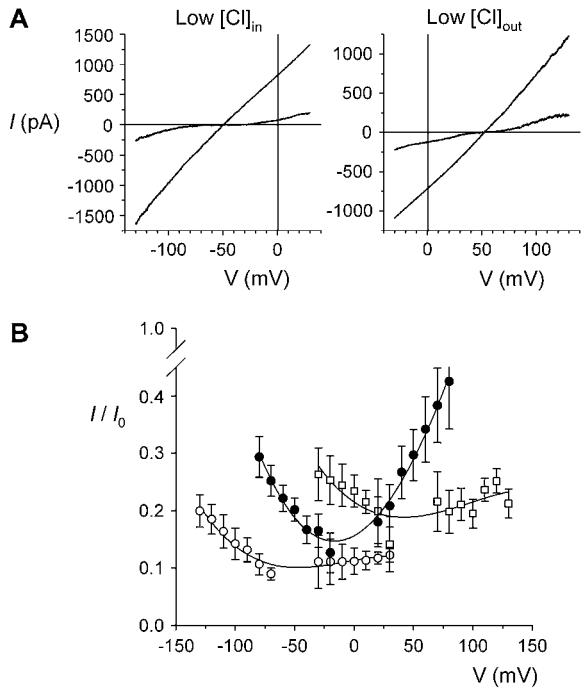

FIGURE 9 Voltage dependence of block of T-338A-CFTR by internal $Au(CN)_2^-$ ions depends on the transmembrane Cl^- gradient. (*A*) Example leak-subtracted I/V relationships recorded from inside out membrane patches. Currents were recorded before and after addition of 1 mM $Au(CN)_2^-$ to the intracellular solution. Chloride concentration was reduced from 154 mM to 24 mM in either the intracellular (*left*) or extracellular (*right*) solution by partial replacement of NaCl by glucose. (*B*) Mean fractional current remaining (i/i_0) after addition of this concentration of $Au(CN)_2^-$ to the intracellular solution, with symmetrical 154 mM Cl^- (●), 24 mM intracellular Cl^- (○), or 24 mM extracellular Cl^- (□). Mean of data from 4–6 patches.

double binding site models shown in Fig. 10. If $Au(CN)_2^-$ is considered as acting at a single site, then the T-338A mutation could increase the rate of $Au(CN)_2^-$ movement between this site and the extracellular solution. This would have the effect of weakening $Au(CN)_2^-$ block from the inside (since $Au(CN)_2^-$ would now better be able to escape its binding site to the extracellular solution, relieving block) and at the same time strengthening block from the outside (since $Au(CN)_2^-$ would now better be able to reach its binding site). In the two binding site model, the effects of the T-338A mutation could result from an increase in the rate of $Au(CN)_2^-$ movement between the two sites. The effect on $Au(CN)_2^-$ block is very similar to that described above for the single site model; intracellular $Au(CN)_2^-$ block is weakened because of enhanced unblock by $Au(CN)_2^-$ permeation to the outside, whereas extracellular $Au(CN)_2^-$ block is strengthened because of increased access to the higher affinity, internal binding site. Note that in both of these suggested models, the effect of the T-338A mutation is to lower a barrier to $Au(CN)_2^-$ movement within the pore, rather than to affect an $Au(CN)_2^-$ binding site. Indeed, for the energy barrier profiles developed (Fig. 10), the effects of the T-338A mutation

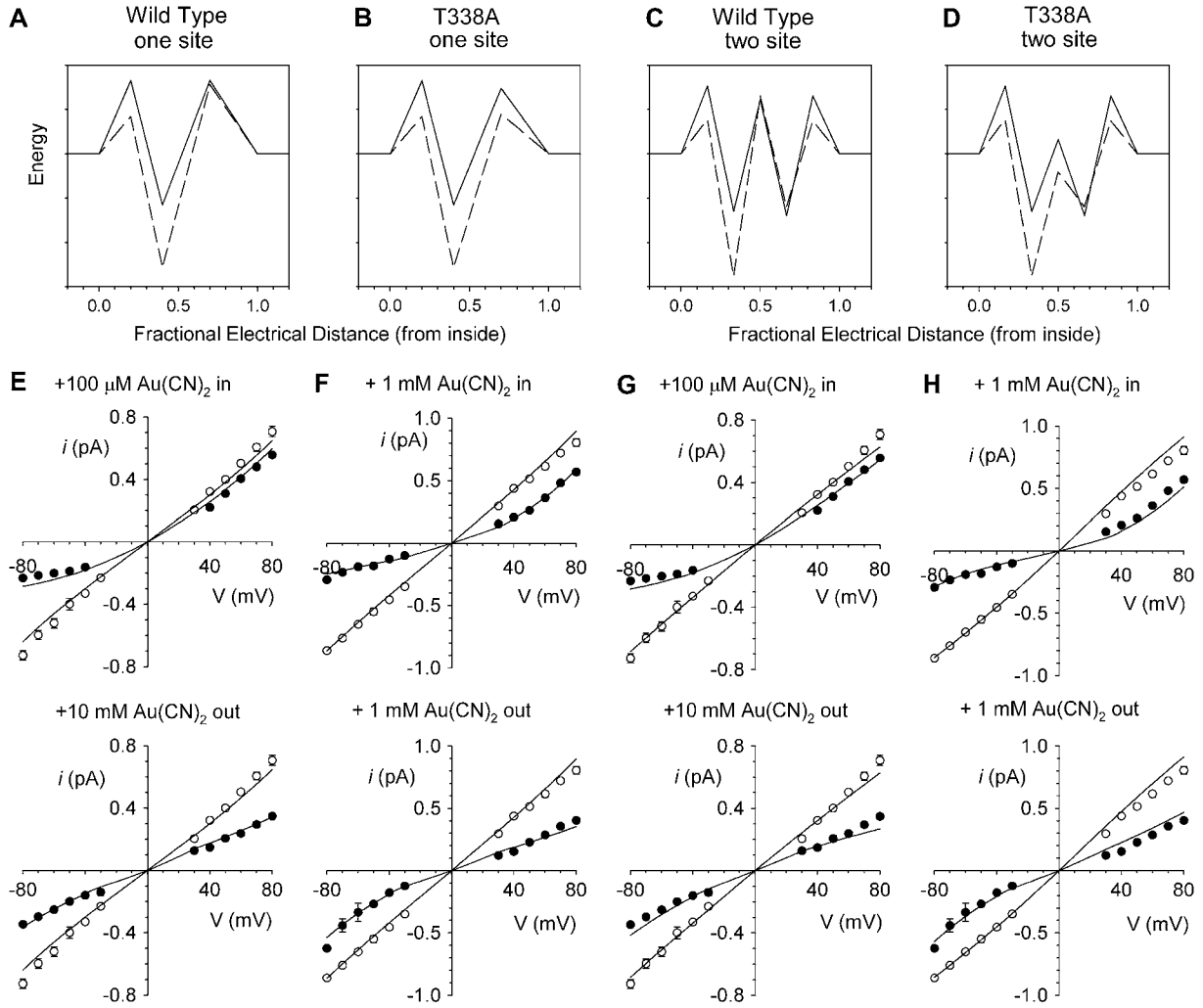

FIGURE 10 Rate theory modeling of Cl^- permeation and $Au(CN)_2^-$ block. (*A–D*) Best fit energy profiles for Cl^- (*solid lines*) and $Au(CN)_2^-$ (*dashed lines*) movement in the CFTR pore. (*A*) One-site model for wild-type. (*B*) One-site model for T-338A. (*C*) Two-site model for wild-type. (*D*) Two-site model for T-338A. To avoid wrongly implying physical meaning to the parameters described by the model, energy is plotted in relative units only. (*E–H*) Predictions of the models shown in *A–D*. Data points for wild-type are taken from Fig. 1, *D* and *E*, and for T-338A from Fig. 4 *A*. In each panel, lines represent the predictions of the model shown above that panel.

are reproduced by lowering the height of a single energy barrier—either the barrier between the binding site and the extracellular solution in the one-site model (Fig. 11 *A*) or the barrier between the two binding sites in the two-site model (Fig. 11 *B*).

The effects of the T-338A mutation are consistent with either the one-site or two-site model (Fig. 11). Indeed, a single binding site model is the simplest that can reproduce the effects of $Au(CN)_2^-$ observed at the single channel level (Fig. 10 *F*). Nevertheless, we would interpret the lack of effect of this mutation on block by either intracellular or extracellular $Pt(NO_2)_4^{2-}$ block as supporting the two-site model, since these data are consistent with the idea that there are blocker binding sites located both external and internal to the location of T-338 within the pore, as illustrated in the two-site model (Fig. 11 *B*).

Voltage and chloride dependence of $Au(CN)_2^-$ block

The voltage dependence of $Au(CN)_2^-$ block is also strongly altered in T-338A-CFTR. In wild-type CFTR, block by intracellular $Au(CN)_2^-$ shows a conventional voltage dependence, with block by this negatively charged substance being strengthened by hyperpolarization of the membrane potential (Figs. 1 *D* and 2 *B*). Block by external $Au(CN)_2^-$ appears to be voltage insensitive (Figs. 1 *E* and 2 *B*), suggesting that the blocker binding site may be outside of the transmembrane electric field. Although some similarities are seen in T-338A (for example, block by internal $Au(CN)_2^-$ is stronger at hyperpolarized than at depolarized voltages; Fig. 4 *C*), the most striking aspect of the voltage dependence of block in this mutant is the ''U''-shaped apparent affinity-voltage

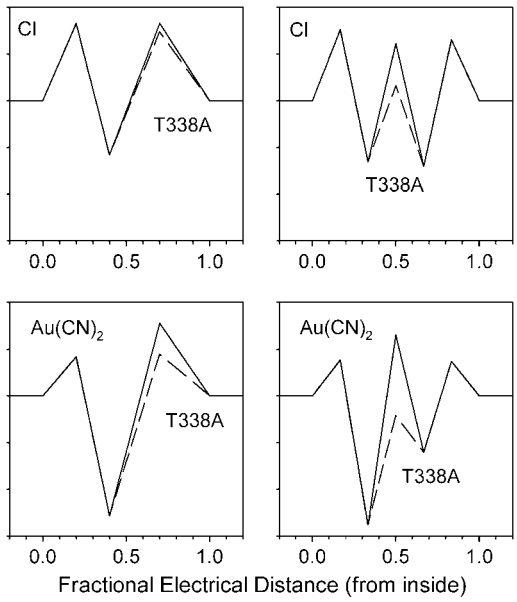

FIGURE 11 Modeling of the effects of the T-338A mutation. Energy profiles shown in Fig. 10 are redrawn to show the effect of the T-338A mutation on Cl^- and $Au(CN)_2^-$ movement in the pore, both for the one-site model (*top*) and the two-site model (*bottom*). In each case, solid lines represent the energy profile for wild-type, and dashed lines the changes made to model T-338A. The effects of the mutation are modeled as (*top*) lowering the energy barrier that exists between the single anion binding site and the extracellular solution, or (*bottom*) lowering the energy barrier that exists between the two anion binding sites. As illustrated in Fig. 10, these localized changes in energy profile were sufficient to model the salient differences in $Au(CN)_2^-$ interactions between wild-type and T-338A.

relationship that characterizes block by both intracellular and extracellular $Au(CN)_2^-$ (Figs. 4 *C* and 5). This unusual relationship between apparent blocker affinity and voltage suggests that block is relieved by both hyperpolarization and by depolarization of the membrane potential, which most likely reflects the ability of the blocking ion to exit either to the extracellular or the intracellular solution. A similar voltage dependence of block is also observed in T-338A-CFTR by the permeant blocking ion SCN^- (Fig. 8) but not the impermeant $Pt(NO_2)_4^{2-}$, which shows a conventional voltage dependence of block when present in the extracellular (Fig. 7) or intracellular solution (19).

Block of wild-type CFTR by intracellular $Au(CN)_2^-$ is strongly influenced by the Cl^- concentration. The affinity of block is greatly decreased and the voltage dependence of block greatly increased as the concentration of Cl^- in the extracellular solution is increased, suggesting that movement of intracellular $Au(CN)_2^-$ and extracellular Cl^- ions are coupled (33). In contrast, intracellular Cl^- has no apparent effect on block by intracellular $Au(CN)_2^-$ (33). In T-338A-CFTR, both intracellular and extracellular Cl^- appear to have a similar impact on block by intracellular $Au(CN)_2^-$, shifting the voltage dependence of block such that the maximum apparent blocker affinity appears to follow the current reversal potential (Fig. 9). This unusual result suggests that $Au(CN)_2^-$ block in this mutant is, in fact, more sensitive to the voltage-dependent flow of Cl^- ions than to the transmembrane voltage itself. Again, this is consistent with the idea that blocking $Au(CN)_2^-$ ions can exit the pore in either direction; at hyperpolarized voltages, rapid Cl^- efflux will sweep blocking $Au(CN)_2^-$ ions from the pore into the extracellular solution, whereas at depolarized potentials Cl^- ions will flow into the intracellular solution and carry blocking $Au(CN)_2^-$ ions along with them.

Role of T-338 as a barrier to anion movement in the pore

Previously we suggested that T-338 contributes to an important lyotropic anion binding site in the pore, based on the finding that the T-338A mutation weakened open channel block by intracellular $Au(CN)_2^-$ ions (21,22). However, this work suggests that this mutation does not in fact affect an $Au(CN)_2^-$ binding site, but instead alters the ability of $Au(CN)_2^-$ to move between different sites within the channel pore. The finding that a point mutation in the pore can have such a large effect on the apparent affinity of a blocker (either increase or decrease) depending on the exact experimental protocol and our suggestion that this occurs without an actual modification of blocker binding sites, therefore, offers an important caveat for site-directed mutagenesis studies that seek to identify blocker binding sites within ion channel pores. Given the different effects of the T-338A mutation on the blocking effects of $Au(CN)_2^-$ and $Pt(NO_2)_4^{2-}$, this caveat might be particularly germane when investigating permeant blockers.

We suggest that the mutation T-338A removes or reduces a barrier to permeant anion movement inside the CFTR channel pore (Fig. 11). The existence of this barrier within the wild-type channel pore appears to play an important role in underlying asymmetric interactions between permeant ions and the pore that result in the strongly asymmetric blocking effects of $Au(CN)_2^-$ (Fig. 2). Removal of this barrier also allows Cl^- ions to effectively sweep blocking $Au(CN)_2^-$ ions from the pore, resulting in a blocking action that is more dependent on voltage-dependent Cl^- flux than on transmembrane voltage itself (Fig. 9). We propose that the barrier associated with T-338 effectively separates the outer and inner pore vestibules, both of which contain permeant anion binding sites with different properties.

It is tempting to speculate that the lyotropic anion binding sites situated external and internal to the T-338 ''barrier'' involve the pore-lining positive charges of R-334 and K-95, respectively. Indeed, of those amino acids that have been studied by site-directed mutagenesis, these two residues have the greatest impact on apparent $Au(CN)_2^-$ binding affinity (22). Furthermore, current models of the pore place these two residues on the extracellular and intracellular side of T-338, respectively (8). Unfortunately, mutagenesis of either of these two positively charged residues causes a considerable

decrease in unitary Cl^- conductance (22,45,46), making single channel studies on the effect of internal and external $Au(CN)_2^-$ ions on these mutants unfeasible. Most other substitutions of T-338 also lead to a large reduction in single channel conductance (26).

CONCLUSIONS

Our results suggest that T-338 contributes to a barrier to anion movement inside the pore. For Cl^- permeation, the consequence of lowering this barrier is an increase in unitary conductance. For anions that interact more strongly with binding sites inside the pore, such as $Au(CN)_2^-$, the existence of a barrier divides the pore into intracellularly and extracellularly accessible compartments, resulting in strongly side-dependent interactions between anions and the channel. Lowering of the barrier, as occurs in the T-338A mutant, results in a channel that interacts much more symmetrically with high affinity permeant anions.

We thank Dr. Osvaldo Alvarez for providing the AJUSTE computer program used for rate theory modeling, and Elizabeth VandenBerg for technical assistance.

This work was supported by the Canadian Institutes of Health Research.

REFERENCES

1. MacKinnon, R. 2003. Potassium channels. *FEBS Lett.* 555:62–65.
2. Dutzler, R. 2004. Structural basis for ion conduction and gating in ClC chloride channels. *FEBS Lett.* 564:229–233.
3. Doyle, D. A., J. M. Cabral, R. A. Pfuetzner, A. Kuo, J. M. Gulbis, S. L. Cohen, B. T. Chait, and R. MacKinnon. 1998. The structure of the potassium channel: molecular basis of K^+ conduction and selectivity. *Science.* 280:69–77.
4. Zhou, Y., J. H. Morais-Cabral, A. Kaufman, and R. MacKinnon. 2001. Chemistry of ion coordination and hydration revealed by a K^+-channel-Fab complex at 2.0 Å resolution. *Nature.* 414:43–48.
5. Dutzler, R., E. B. Campbell, and R. MacKinnon. 2003. Gating the selectivity filter in ClC chloride channels. *Science.* 300:108–112.
6. Sather, W. A., and E. W. McCleskey. 2003. Permeation and selectivity in calcium channels. *Annu. Rev. Physiol.* 65:133–159.
7. Chen, T.-Y. 2005. Structure and function of CLC channels. *Annu. Rev. Physiol.* 67:809–839.
8. Linsdell, P. 2006. Mechanism of chloride permeation in the cystic fibrosis transmembrane conductance regulator chloride channel. *Exp. Physiol.* 91:123–129.
9. Hille, B. 2001. Ion Channels of Excitable Membranes, 3rd ed. Sinauer Associates, Sunderland, MA.
10. Neyton, J., and C. Miller. 1988. Potassium blocks barium permeation through a calcium-activated potassium channel. *J. Gen. Physiol.* 92: 549–567.
11. Neyton, J., and C. Miller. 1988. Discrete Ba^{2+} block as a probe of ion occupancy and pore structure in the high-conductance Ca^{2+}-activated K^+ channel. *J. Gen. Physiol.* 92:569–586.
12. Dawson, D. C., S. S. Smith, and M. K. Mansoura. 1999. CFTR: mechanism of anion conduction. *Physiol. Rev.* 79:S47–S75.
13. Linsdell, P. 2001. Thiocyanate as a probe of the cystic fibrosis transmembrane conductance regulator chloride channel pore. *Can. J. Physiol. Pharmacol.* 79:573–579.
14. Tabcharani, J. A., J. M. Rommens, Y.-X. Hou, X.-B. Chang, L.-C. Tsui, J. R. Riordan, and J. W. Hanrahan. 1993. Multi-ion pore behaviour in the CFTR chloride channel. *Nature.* 366:79–82.
15. Mansoura, M. K., S. S. Smith, A. D. Choi, N. W. Richards, T. V. Strong, M. L. Drumm, F. S. Collins, and D. C. Dawson. 1998. Cystic fibrosis transmembrane conductance regulator (CFTR) anion binding as a probe of the pore. *Biophys. J.* 74:1320–1332.
16. Gupta, J., A. Evagelidis, J. W. Hanrahan, and P. Linsdell. 2001. Asymmetric structure of the cystic fibrosis transmembrane conductance regulator chloride channel pore suggested by mutagenesis of the twelfth transmembrane region. *Biochemistry.* 40:6620–6627.
17. Linsdell, P. 2001. Relationship between anion binding and anion permeability revealed by mutagenesis within the cystic fibrosis transmembrane conductance regulator chloride channel pore. *J. Physiol.* 531:51–66.
18. Smith, S. S., E. D. Steinle, M. E. Meyerhoff, and D. C. Dawson. 1999. Cystic fibrosis transmembrane conductance regulator. Physical basis for lyotropic anion selectivity patterns. *J. Gen. Physiol.* 114:799–818.
19. Gong, X., and P. Linsdell. 2003. Mutation-induced blocker permeability and multiion block of the CFTR chloride channel pore. *J. Gen. Physiol.* 122:673–687.
20. Liu, X., S. S. Smith, and D. C. Dawson. 2003. CFTR: what's it like inside the pore? *J. Exp. Zool.* 300A:69–75.
21. Gong, X., S. M. Burbridge, E. A. Cowley, and P. Linsdell. 2002. Molecular determinants of $Au(CN)_2^-$ binding and permeability within the cystic fibrosis transmembrane conductance regulator Cl^- channel pore. *J. Physiol.* 540:39–47.
22. Ge, N., C. N. Muise, X. Gong, and P. Linsdell. 2004. Direct comparison of the functional roles played by different transmembrane regions in the cystic fibrosis transmembrane conductance regulator chloride channel pore. *J. Biol. Chem.* 279:55283–55289.
23. Gong, X., and P. Linsdell. 2003. Molecular determinants and role of an anion binding site in the external mouth of the CFTR chloride channel pore. *J. Physiol.* 549:387–397.
24. Serrano, J. R., X. Liu, E. R. Borg, C. S. Alexander, C. F. Shaw, and D. C. Dawson. 2006. CFTR: ligand exchange locks a permeant anion in the pore. *Biophys. J.* 91:1737–1748.
25. Ge, N., and P. Linsdell. 2006. Interactions between impermeant blocking ions in the cystic fibrosis transmembrane conductance regulator chloride channel pore: evidence for anion-induced conformational changes. *J. Membr. Biol.* 210:31–42.
26. Linsdell, P., S.-X. Zheng, and J. W. Hanrahan. 1998. Non-pore lining amino acid side chains influence anion selectivity of the human CFTR Cl^- channel expressed in mammalian cell lines. *J. Physiol.* 512:1–16.
27. McCarty, N. A., and Z.-R. Zhang. 2001. Identification of a region of strong discrimination in the pore of CFTR. *Am. J. Physiol.* 281: L852–L867.
28. Cheung, M., and M. H. Akabas. 1996. Identification of cystic fibrosis transmembrane conductance regulator channel-lining residues in and flanking the M6 membrane-spanning segment. *Biophys. J.* 70: 2688–2695.
29. Liu, X., Z.-R. Zhang, M. D. Fuller, J. Billingsley, N. A. McCarty, and D. C. Dawson. 2004. CFTR: a cysteine at position 338 in TM6 senses a positive electrostatic potential in the pore. *Biophys. J.* 87:3826–3841.
30. Liu, X., C. Alexander, J. Serrano, E. Borg, and D. C. Dawson. 2006. Variable reactivity of a cysteine at position 338 in cystic fibrosis transmembrane conductance regulator reflects different chemical states of the thiol. *J. Biol. Chem.* 281:8275–8285.
31. Gong, X., S. M. Burbridge, A. C. Lewis, P. Y. D. Wong, and P. Linsdell. 2002. Mechanism of lonidamine inhibition of the CFTR chloride channel. *Br. J. Pharmacol.* 137:928–936.
32. Gupta, J., and P. Linsdell. 2002. Point mutations in the pore region directly or indirectly affect glibenclamide block of the CFTR chloride channel. *Pflugers Arch.* 443:739–747.
33. Gong, X., and P. Linsdell. 2003. Coupled movement of permeant and blocking ions in the CFTR chloride channel pore. *J. Physiol.* 549: 375–385.

34. Linsdell, P., and J. W. Hanrahan. 1996. Disulphonic stilbene block of cystic fibrosis transmembrane conductance regulator Cl^- channels expressed in a mammalian cell line and its regulation by a critical pore residue. *J. Physiol.* 496:687–693.

35. Linsdell, P., and J. W. Hanrahan. 1998. Adenosine triphosphate-dependent asymmetry of anion permeation in the cystic fibrosis transmembrane conductance regulator chloride channel. *J. Gen. Physiol.* 111: 601–614.

36. Alvarez, O., A. Villarroel, and G. Eisenman. 1992. Calculation of ion currents from energy profiles and energy profiles from ion currents in multibarrier, multisite, multioccupancy channel model. *Methods. Enzymol.* 207:816–854.

37. Linsdell, P., J. A. Tabcharani, and J. W. Hanrahan. 1997. Multi-ion mechanism for ion permeation and block in the cystic fibrosis transmembrane conductance regulator chloride channel. *J. Gen. Physiol.* 110:365–377.

38. Linsdell, P., and X. Gong. 2002. Multiple inhibitory effects of $Au(CN)_2^-$ ions on cystic fibrosis transmembrane conductance regulator Cl^- channel currents. *J. Physiol.* 540:29–38.

39. Wright, A. M., X. Gong, B. Verdon, P. Linsdell, A. Mehta, J. R. Riordan, B. E. Argent, and M. A. Gray. 2004. Novel regulation of cystic fibrosis transmembrane conductance regulator (CFTR) channel gating by external chloride. *J. Biol. Chem.* 279:41658–41663.

40. Linsdell, P. 2005. Location of a common inhibitor binding site in the cytoplasmic vestibule of the cystic fibrosis transmembrane conductance regulator chloride channel pore. *J. Biol. Chem.* 280:8945–8950.

41. Sheppard, D. N., and K. A. Robinson. 1997. Mechanism of glibenclamide inhibition of cystic fibrosis transmembrane conductance regulator Cl^- channels expressed in a murine cell line. *J. Physiol.* 503: 333–346.

42. Zhou, Z., S. Hu, and T.-C. Hwang. 2002. Probing an open CFTR pore with organic anion blockers. *J. Gen. Physiol.* 120:647–662.

43. McCarty, N. A. 2000. Permeation through the CFTR chloride channel. *J. Exp. Biol.* 203:1947–1962.

44. Muanprasat, C., N. D. Sonawane, D. Salinas, A. Taddei, L. J. V. Galietta, and A. S. Verkman. 2004. Discovery of glycine hydrazide pore-occluding CFTR inhibitors. Mechanism, structure-activity analysis, and in vivo efficacy. *J. Gen. Physiol.* 124:125–137.

45. Smith, S. S., X. Liu, Z.-R. Zhang, F. Sun, T. E. Kriewall, N. A. McCarty, and D. C. Dawson. 2001. CFTR: covalent and noncovalent modification suggests a role for fixed charges in anion conduction. *J. Gen. Physiol.* 118:407–431.

46. Gong, X., and P. Linsdell. 2004. Maximization of the rate of chloride conduction in the CFTR channel pore by ion-ion interactions. *Arch. Biochem. Biophys.* 426:78–82.